ACS APPLIED MATERIALS & INTERFACES

RESEARCH ARTICLE

www.acsami.org

Synthesis and Development of a Multifunctional Self-Decontaminating Polyurethane Coating

James H. Wynne,*[,†] Preston A. Fulmer,[†] D. Michelle McCluskey,[‡] Nicole M. Mackey,[‡] and J. Paige Buchanan[‡,§]

[†]Chemistry Division, Naval Research Laboratory, 4555 Overlook Avenue SW, Code 6100, Washington, D.C. 20375, United States

[‡]Department of Chemistry and Biochemistry, University of Southern Mississippi, 118 College Drive, Hattiesburg, Mississippi 39406, United States

ABSTRACT: A unique, durable, nonleaching antimicrobial urethane coating possessing energy-dampening properties is reported. Five novel diol-functionalized quaternary ammonium bromide salts were designed, synthesized, and cross-linked with a commercial polyisocyanate to afford novel multifunctional self-decontaminating coatings. Leaching of the antimicrobial into the environment is eliminated because of the biocidal tether. The effectiveness of these molecules to self-concentrate at the air−polymer interface without addition of other surface modifying additives proved extremely advantageous, and consequently resulted in microphase separation as confirmed by AFM. The coatings were designed to continuously decontaminate against a variety of pathogenic bacteria in addition to affording preliminary dampening properties. Minimum inhibitory concentration studies as well as surface antimicrobial evaluations were conducted using both Gram-positive and Gram-negative bacteria. Additionally, viscoelastic properties, hardness, tack, and surface energy measurements were used to correlate with coating performance.

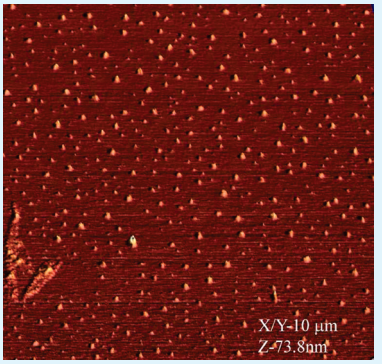

KEYWORDS: additives, antimicrobial, biocide, coating, self-decontaminating surfaces, dampening

1. INTRODUCTION

With the increase in antibiotic resistant microbes, there has been an explosion of interest in the development of novel coatings that are capable of self-decontaminating against a variety of pathogenic bacteria.[1,2] Such surfaces, when incorporated into commercial products such as children's toys,[3] medical devices,[4−6] and hospital surfaces,[7,8] could reduce the number of infections caused by pathogenic bacteria. A number of active components for self-decontaminating surfaces have been investigated, including common antibiotics,[9,10] silver ions,[4−6] antimicrobial peptides,[11−13] and quaternary ammonium salts.[14−16]

The search for biocides with improved antimicrobial and functional performance has led to the development of several generations of cationic quaternary ammonium salts (QAS) which are widely used for the control of bacterial growth in clinical, industrial and marine environments.[17] Quaternary ammonium salts have been used as key components in many disinfectants, fabric softeners, laundry detergents, and antistatic agents.[17,18] QAS have high biocidal activity for a wide spectrum of biological species at minimal concentrations and can be easily tailored for desired functionality and alkyl chain length through traditional chemical synthesis.[15,16,19] Varying the functionality by incorporating polymerizable functional groups allows QAS to be cross-linked into nonleaching biocidal coatings,[20,21] with high antimicrobial activity against a wide range of bacteria, molds, and yeast.[15,19,22,23] The accepted mode of action of QAS biocides is described briefly as follows.[24,25] The QAS polymer surface creates a strong electrostatic interaction with bacteria. Once the bacteria are adhered to the surface, the QAS's hydrophobic alkyl chain diffuses through the bacteria's cell wall and disrupts the cytoplasmic membrane, causing cell death. Alkyl chain length plays a critical role in biocidal activity of the QAS. Several studies have shown that QASs with alkyl chain lengths longer than C8 have increased biocidal activity.[26,27]

Urethane systems have been studied extensively in a wide range of fields and are shown to be an extremely versatile resin system. Furthermore, isocyanates are commercially available with numerous structural characteristics allowing the possibility of tailored molecular architecture.[28,29] The ease of preparation of OH terminated biocidal monomers allows for the straightforward formation of urethane bonds through the reaction of primary alcohols with various isocyanates. Urethanes are known to have excellent impact strength, low curing temperature, and abrasion resistant characteristics.[30] Potential end-use applications for biocide containing urethane systems include foams, coatings, medical devices, food packaging, textiles, and building materials.[30,31]

Noise vibration travels via two mechanisms: through space (e.g., air or water) and transmission through the substrate. Dampening coatings act by attenuating the noise vibration signal prior to its release from the substrate, converting the energy into low grade heat. Many industries have taken advantage of the excellent coating properties of urethanes and applied them to

Received: February 28, 2011
Accepted: May 5, 2011
Published: May 05, 2011

noise dampening applications such as wood flooring.[32] Viscoelastic properties are investigated to determine the parameters of the dampening property. Urethane coatings can be tailored to express dampening properties over a specific temperature range by manipulating the glass transition temperature (T_g) resulting in a multifunctional coating with excellent coating properties and sound dampening attributes.

Coatings presenting a surface free of microorganisms would be extremely advantageous for sanitary reasons such as in health care fields and food preparation areas, but would also have immediate use in marine environments where fouling by microorganisms increases ship drag and fuel consumption resulting in increased costs and reduced efficiency.[33,34] The goal of the present work is to synthesize antimicrobial quaternary ammonium diols, which when cross-linked with a polyisocyanate afford a polyurethane coating system characterized by a significant enhancement of antimicrobial activity at the coating-air interface and show promise for room temperature dampening as indicated by dynamic mechanical analysis screening tests. A durable, nonleaching antimicrobial and potentially energy-dampening coating is extremely desirable and is the subject of this report.

2. EXPERIMENTAL SECTION

All chemicals were of reagent grade and used without additional purification with the exception of THF and toluene. THF was distilled from sodium/benzophenone, and toluene was distilled from sodium, both under nitrogen. Moisture sensitive reactions were conducted in oven-dried glassware under a nitrogen atmosphere. Unless otherwise noted, ^{1}H and ^{13}C NMR were taken in $CDCl_3$ at 300 and 60 MHz respectfully, with TMS internal standard. Chemical shifts were reported in units of ppm downfield from TMS.

Reaction parameters for the synthesis of QAS-diols (**3**) were optimized using a ThermoFisher LXQ Ion-trap MS and Accela HPLC system (Hypersil Gold reverse phase column of dimensions 50 mm × 2.1 mm, ethanol as eluent, and hexadecyltrimethyl ammonium bromide (Aldrich, 98%) as internal standard). QAS-diols were isolated as pure compounds and combined with Desmodur N 3600^{TM}, a polyfunctional isocyanate provided by Bayer Inc., to form reactive prepolymers. This aliphatic polyisocyanate was selected for its compatibility with the ammonium compounds employed in this study. Films were prepared from prepolymer solutions according to the specific method reported; however, in general, films were drawn onto substrates using a #52 draw-down bar wet-film applicator. Aluminum Q-panel^{TM} test panels and the wet-film applicator were purchased from Paul N. Gardner Company, Inc. (Pompano Beach, FL). Prepared films were rinsed with deionized water three times and rinsewater analyzed by HPLC to ensure quaternary ammoniums were not leaching from the films.

General Procedure for Preparation of 3. Into a 50 mL, round-bottomed flask, equipped with reflux condenser and a positive flow of nitrogen, were placed *N*-methyl aminodiethanol (**2**) (20 mmol), bromoalkane (**1**) (20 mmol), and absolute ethanol (EtOH, 15 mL). The solution was refluxed for 24 h. After slowly being cooled to room temperature, the crude sample was concentrated under reduced pressure. The resulting thick yellow solid was tirtrated with petroleum ether (2 × 3 mL) and placed under a vacuum to remove trace solvent. The resulting product was then recrystallized from ethanol to afford the desired product (**3**).

Butyl bis(2-hydroxyethyl)methyl ammonium bromide (**3a**): FTIR: 3310, 2960, 2867, 1687, 1466, 1231, 1085, 977, 911, 734 cm^{-1}. ^{1}H NMR ($CDCl_3$): 5.13 (m, 2H), 4.01 (m, 4H), 3.73−3.65 (t, J = 7, 4H), 3.62−3.58 (t, J = 6, 2H), 3.31 (s, 3H), 1.82−1.72 (q, 2H), 1.44−1.34 (m, 2H), 0.99 (t, J = 6, 3H) δ. ^{13}C NMR ($CDCl_3$): 64.2, 63.9, 55.9, 50.3, 42.0, 24.5, 19.8, 13.9 δ.

Hexyl bis(2-hydroxyethyl)methyl ammonium bromide (**3b**): FTIR: 3306, 2956, 2921, 2864, 1458, 1366, 1254, 1085, 1046, 950, 730 cm^{-1}. ^{1}H NMR ($CDCl_3$): 4.93−4.90 (m, 2H), 4.05 (m, 4H), 3.75−3.73 (m, 4H), 3.71−3.68 (m, 2H), 3.31 (s, 3H), 1.78 (m, 2H), 1.34 (m, 6H), 0.92−0.89 (t, J = 6, 3H) δ. ^{13}C NMR ($CDCl_3$): 63.8, 58.8, 55.6, 50.0, 30.9, 25.7, 22.2, 22.1, 13.7 δ.

Octyl bis(2-hydroxyethyl)methyl ammonium bromide (**3c**): FTIR: 3310, 2952, 2925, 2860, 1628, 1466, 1366, 1254, 1085, 1046, 965, 719 cm^{-1}. ^{1}H NMR ($CDCl_3$): 5.19 (m, 2H), 4.13−4.11 (m, 4H), 3.67−3.65 (m, 4H), 3.58−3.52 (m,2H), 3.29 (s, 3H), 1.76 (m, 2H), 1.34−1.27 (m, 10H), 0.90−0.86 (t, J = 5.5, 3H) δ. ^{13}C NMR ($CDCl_3$): 63.8, 57.9, 55.6, 49.9, 31.5, 28.9, 26.1, 22.4, 22.3, 14.0 δ.

Decyl bis(2-hydroxyethyl)methyl ammonium bromide (**3d**): FTIR: 3310, 2958, 2921, 2850, 1470, 1375, 1269, 1088, 952 cm^{-1}. ^{1}H NMR ($CDCl_3$): 4.80−4.77 (m, 2H), 4.11−4.10 (m, 4H), 3.74−3.73 (m, 4H), 3.57−3.52 (m, 2H), 3.33 (s, 3H), 1.75 (m, 2H), 1.35−1.26 (m, 14H), 0.90−0.85 (t, J = 6, 3H) δ. ^{13}C NMR ($CDCl_3$): 64.2, 58.2, 55.7, 50.5, 31.8, 29.4, 29.2, 26.4, 22.6, 14.1 δ.

Octadecyl bis(2-hydroxyethyl)methyl ammonium bromide (**3e**): FTIR: 3291, 2918, 2850, 1482, 1464, 1085, 1050, 1033, 1018, 913, 626 cm^{-1}. ^{1}H NMR ($CDCl_3$): 4.75−4.72 (m, 2H), 4.14−4.10 (m, 4H), 3.84−3.78 (m, 4H), 3.59−3.55 (m, 2H), 3.34 (s, 3H), 1.73 (m, 2H), 1.36−1.26 (m, 30H), 0.91−0.87 (t, J = 6, 3H) δ. ^{13}C NMR ($CDCl_3$): 64.0, 59.6, 55.8, 52.2, 31.9, 29.7, 29.6, 29.5, 29.3, 29.2, 26.4, 14.4 δ.

General Procedure for the Preparation and Application of Prepolymers 5 and 6. Into a 50-mL, round-bottom flask equipped with reflux condenser and stir bar were placed 2 mL of *N*-methylpyrrolidone (NMP) and 5.5 mmol of either *N*-methyl aminodiethanol (**2**) or *N*-alkyl derivative of *N*-methyl aminodiethanol (**3**) respectively. A 2.0 g aliquot of Desmodur N3600 (ca. 11.0 mmol equivalent of −NCO) was added to the mixture and stirred for 4 h at 60 °C. The respective viscous, transparent, homogeneous mixtures were afforded as partially cross-linked prepolymers **5** and **6**, respectively.

The prepolymers (**5** and **6**) were applied onto both Q-panels and glass microscope slides using the draw-down bar. After 6 h of curing at 120 °C, faint yellow transparent and visually uniform films were achieved. Additional drying time was employed to remove residual solvents during cure. Q-panels were coated for hardness and tack measurements. Similarly, 1.5−2.0 g samples were prepared in 2 in. cylindrical silicone dishes, which afforded flexible and elastic polymer disks. These samples were used for DMA, TGA, DSC, gel fraction, and antimicrobial analyses.

Film Tack, Hardness, and Contact Angle Measurements. Film tack and hardness measurements were performed using a TA XTplus Texture Analyzer (Godelming, Surrey, UK). Using compression test mode, the applied load required to penetrate 10% of the film thickness with a one inch round probe tip at a probe insertion speed of 0.1 mm/sec was determined for each sample. In tack measurements, the probe tip and applied load was held for 10 s and then withdrawn at a constant rate (0.1 mm/sec) from the film. Tack measurements were recorded as grams per unit time, with the highest point recorded as the peak tack. Liquid contact angles were measured at 20 °C using a VCA 2500-AST goniometer, equipped with a light source, camera, and flat horizontal support for test slides. Water drops of 5 μL were deposited on samples, and static contact angles calculated. Reported contact angles were determined as the average of three measurements per slide. All measurements, from both drop sides, were compared and found to be equal within experimental error.

Mechanical and Thermal Analysis and Gel Factions. Glass transition temperatures (T_g) of prepared polymer samples were measured using a Perkin-Elmer DMA Model 8000 Dynamic Mechanical Analysis (DMA) instrument. Cured samples were cut into rectangular

test samples, 30 mm length and 5 mm width, with thickness varying slightly from sample to sample. Samples were tested in tension mode, frequency 1 Hz, amplitude 15 μm, over the temperature range of −70 to 150 °C, with a ramp rate of 2 °C/min. T_g was approximated as the peak of the tan delta (δ) plot. Gel fractions of the cured films were obtained by dissolving a known mass of film in toluene, resting the sample for 24 h at room temperature, and recovering the insoluble mass fraction, followed by residual solvent evaporation under reduced pressure. The thermal stability of cured polymer samples was evaluated by thermogravimetric analysis (TGA). Using a TA Instruments Q500 series TGA instrument, 5−10 mg samples were analyzed over the temperature range of 0−600 °C at a heating rate of 10 °C/min. The atomic force microscope (AFM) measurement was performed with a Nanoscope IIIa (Veeco Instruments, Inc.) operating in the tapping mode. Commercial ultrasharp, rectangular silicon cantilevers made by Micromasch (250 × 35 × 1.7 μm^3) were used having a nominal spring constant of~0.35 N/m and a resonance frequency of ~33 kHz.

Bacterial Challenges. *Bacteria and Media.* Luria−Bertani (LB) media (Difco Laboratories, Detroit, MI) was used as a bacterial growth medium for preparation of bacteria for bacterial challenges, and Letheen broth (Difco Laboratories, Detroit, MI) was used as a growth medium postchallenge, due to its ability to inactivate quaternary ammonium salts. Both were prepared according to the manufacturer's specifications. *Staphylococcus aureus* (ATCC 25923) was used for all Gram-positive bacterial challenges. *Escherichia coli* (ATCC 11105) was used for all Gram-negative bacterial challenges. Log phase cultures were grown in LB media, pelleted, and resuspended in a 0.5% saline solution.

MIC Studies. To determine the minimum inhibitory concentration (MIC) of antimicrobial compounds, were weighed synthesized biocides and dissolved then in sterile water. Each compound was then added to Luria−Bertani (LB) media at varying concentrations. To the mixture of LB and biocide was added 1 × 10^7 CFU of *Staphylococcus aureus* (ATCC 25923) for Gram-positive tests or *Escherichia coli* (ATCC 11105) for Gram-negative tests. Cultures were then incubated for 18 h at 37 °C and examined visually for turbidity. MIC was determined to be the lowest concentration of biocide that prevented visible bacterial growth at 18 h.

Coating Studies. As described previously, a 10 μL aliquot of 10^9 CFU/mL log phase bacteria were added to 1 cm^2 area of each test sample.[13,14] To prevent desiccation, samples were placed in a hydration chamber consisting of a sterile Petri dish containing a sterile 2 × 2 in. gauze pad wetted with 2 mL of sterile H_2O. The bacteria were exposed at room temperature for 2 h. The coatings were then swabbed with a sterile cotton swab, which was then placed in 5 mL of Letheen broth and vortexed vigorously to suspend the bacteria evenly throughout the broth. The broth was then serially diluted seven times. The dilutions were incubated at 37 °C for 18 h, visually examined, and determined to have growth by the presence of turbidity. Log kill was determined by the following formula: 7 − highest dilution exhibiting bacterial growth = Log kill.

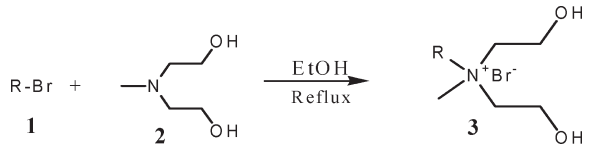

Figure 1. Synthetic scheme of quaternary ammonium salt diol (QAS-diol).

3. RESULTS AND DISCUSSION

Our primary objective was to synthesize a series of quaternary ammonium diols with varied alkyl length, Figure 1, and evaluate their biocidal activity against both Gram-positive and Gram−negative bacteria in solution studies and in films. Through the hydroxyl (OH) functionality of the QAS-diol, these biocides are readily incorporated into cross-linked thermoset resins using a commercial isocyanate, such as Desmodure N 3600, an aliphatic polyisocyanate prepolymer resin based on hexamethylene di-isocyanate (HDI), Figure 2. A critical parameter for this study was to determine the extent of biological activity of agents present as resin matrix components when compared to the more common solution minimum inhibitory concentration (MIC) studies. In film studies, the question of biological activity is reduced to a two-dimensional reaction environment, where surface energy considerations are paramount.

MIC assays, Table 1, for the series of QAS-diols (**3**) suggests that compounds of higher alkyl chain length (C-8, C-10 and C-18) possess significant biocidal activity. MIC defines the minimum concentration of biocidal agent that will inhibit the visible growth of a microorganism over an 18 h incubation. MIC values for QAS diols (**3c**−**3e**) were <0.347, <0.038, <0.023 and <0.70, <0.092, <0.230 μg/L for *S. aureus* and *E. coli*, respectively, and were very similar to those reported for other QASs.[15] Therefore these agents were cured with commercial isocyanate resin (Desmodur N 3600) at a 1:1 mol equiv of OH:NCO groups to obtain polyurethane resins chemically incorporating the biocide into the polymer matrix. A control film was also prepared from *N*-methyl aminodiethanol and hardener, according to Figure 3. In the semiquantitiative film assay developed in our lab, the biocidal activity is read as a log reduction in kill as evidenced by the presence or absence of turbidity from a starting point concentration of 1 × 10^7 CFU/cm^2.[35,36] Control films presented no biocidal activity, and C8−C18 exhibited a 3 log reduction of *S. aureus*. An interesting reversal of agent order

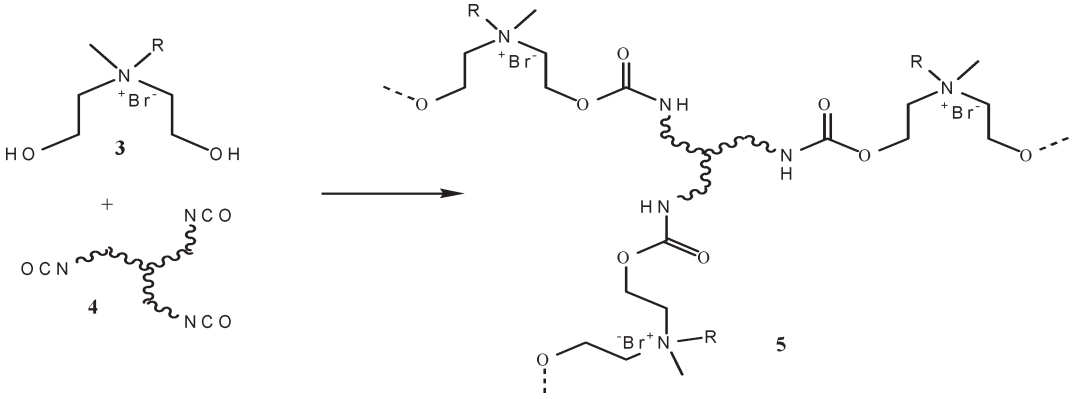

Figure 2. Synthesis of quaternary ammonium salt urethane network (QAS-urethane).

Table 1. Minimum Inhibitory Concentrations (MIC) and Surface Biocidal Activity for Synthesized Quaternary Ammonium Compounds (QAS-diols) and Their Respective Polyurethane Thermoset Resins (QAS-urethanes)

			solution results			coating results	
sample ID	(1) R	yield (%)	*S. aureus* Gram (+) MIC (μg/L)	*E. coli* Gram (−) MIC (μg/L)	sample ID	*S. aurus* Gram (+)[a]	*E. coli* Gram (−)[a]
2			>10	>10	**6**	0 log	0 log
3a	nC_4H_9-	91	3.6	>10	**5a**	0 log	0 log
3b	nC_6H_{13}-	89	6.48	>10	**5b**	0 log	0 log
3c	nC_8H_{17}-	93	<0.347	<0.70	**5c**	3 log	5 log
3d	$nC_{10}H_{21}$-	92	<0.038	<0.092	**5d**	3 log	2 log
3e	$nC_{18}H_{37}$-	91	<0.023	<0.230	**5e**	3 log	1 log

[a] Reported in log reduction from a starting point concentration of 1×10^7CFU/cm^2.

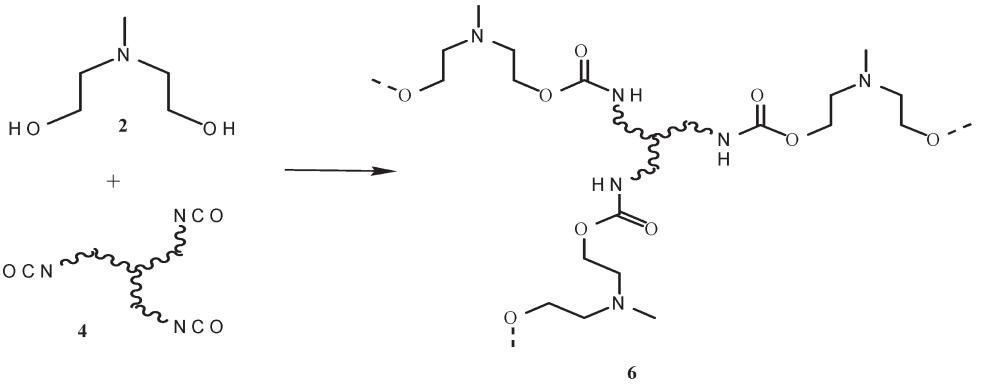

Figure 3. Synthesis of nonquaternized polyurethane control system.

resulted when considering the activity of film-bound agents against *E. coli*, where MIC results suggested that increasing alkyl-chain length results in an increase in biocidal activity. In film studies, C8 alkyl chain QAS-urethane networks possessed enhanced activity relative to C18 derivatives. The polymerization process used in this work, where the biocide is incorporated into the urethane network as a reactive monomer and not as an additive, would ideally produce a coating having uniformly dispersed biocide provided that the reagents remain miscible and complete cure occurs. To account for the increased biocidal activity of the C8 alkyl films over their C18 analogs, a difference in the surface properties must exist that leads to the reduced activity of the more lethal C18 derivative once it is incorporated into a film. For the films to be biocidal, bacteria must be surface bound and interact with the quaternary ammonium film constituent. In the case of longer alkyl chain lengths, a shielding of the electrostatic attractive forces of the quaternary ammonium compound may result. The supporting characterization of film surface properties, as well as physical and mechanical testing, was performed on cured samples using a combination of techniques and presented in Tables 2 and 3.

Water contact angles and texture analysis characterized the surface properties, which are summarized in Table 2. Water contact angles were obtained from samples cast on aluminum coupons and found to be independent of composition. Contact angles of ~70° suggest that the coatings (**5c**−**e**) possess balanced hydrophilicity/hydrophobicity characteristics. Prepared films were considered hard as determined by texture analysis, and all films were found to give comparable results within experimental error. For comparison, a soft film possessing a ~20 g film hardness value using texture analysis was recently

Table 2. Surface Properties: Film Hardness, Tack, and Water Contact Angle of Cured Biocidal Urethane Resins (QAS-urethanes)

sample ID	R	tack (g)[a,b]	hardness (g)[a,c]	contact angle (deg)[a]
5c	nC_8H_{17}-	113 (±19)	70 (±8)	70 (±1.5)
5d	$nC_{10}H_{21}$-	85 (±11)	93 (±9)	70 (±0.5)
5e	$nC_{18}H_{37}$-	46 (±11)	51 (±11)	73 (±0.4)
6		35 (±15)	63 (±10)	71 (±0.1)

[a] Average of >6 measurements are reported with (standard deviations), prepared 1:1 OH:NCO using Desmodur N 3600. [b] Maximum on mass/time tack plot. [c] Force required to penetrate 10% thickness of coating with a 1 in. stainless steel probe tip.

reported for a ~70.0 wt % polydimethylsiloxane (PDMS) containing, amine-cured epoxy system.[19] Hardness values obtained on samples were used in the tack test, where the force required to debond the probe tip from a 10% coating depth at a constant rate is obtained in grams/unit time, and the highest point on the tack versus time plot is reported as the peak tack. Contrary to hardness and contact angle measurements, which showed no trend with composition and were "typical" for polymers, tack values were relatively large for the series and decreased with increasing alkyl chain length. The octyl derivative (**5c**) had the highest tack. This interesting result is attributed to the reduced screening (cloaking) of the positively charged ammonium group by the shorter alkyl chain length. Conversely, the lowest tack was observed in the unquaternized polymer network consistent with the concept that ammonium charge underlies tack in these materials. Tack data correlates well with

Table 3. Mechanical Properties, Extent of Cross-Linking, and Thermal Stability of Cured Biocidal-Urethane Resins

sample ID	R	gel fraction (%)[a]	tan δ maximum[b]	T_{g1} (°C)[c]	T_{g2} (°C)[c]	degradation onset (°C)[d]
5c	nC_8H_{17}-	90.9	0.68	−3.5		200.6
5d	$nC_{10}H_{21}$-	89.6	0.68	−1.3		189.3
5e	$nC_{18}H_{37}$-	90.5	0.56	11.5	32.2	178.9
6		88.7	0.68	0.6		230.0

[a] Gel fraction quantified as the insoluble fraction recovered after 24 h solvent exposure. [b] Maximum damping in tan δ plot. [c] T_g recorded as the temperature corresponding to the peak maxima of tan δ plot. [d] Temperature corresponding to 10 wt % mass loss, heating rate of 10 °C/min in nitrogen.

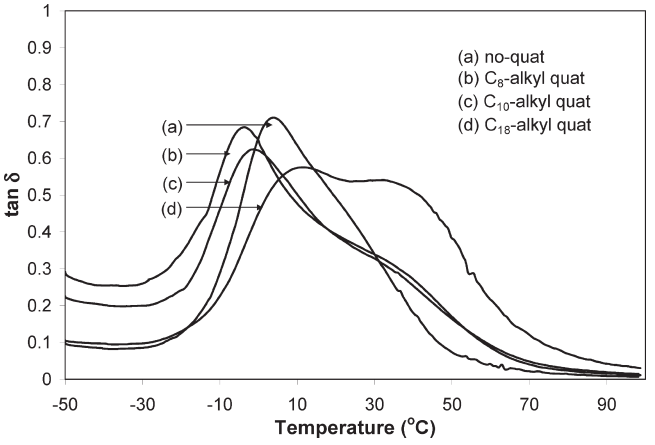

Figure 4. DMA analysis of prepared biocidal-urethane coatings, showing glass transitions (T_g) as the peak of the tan delta plot.

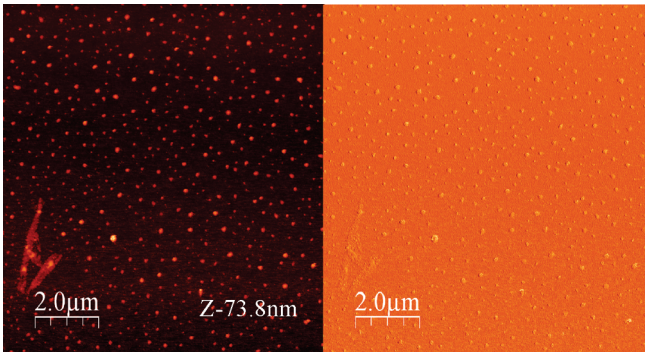

Figure 5. AFM analysis of C18-alkyl QAS-urethane films; (left) height (73.8 nm) and (right) phase plots.

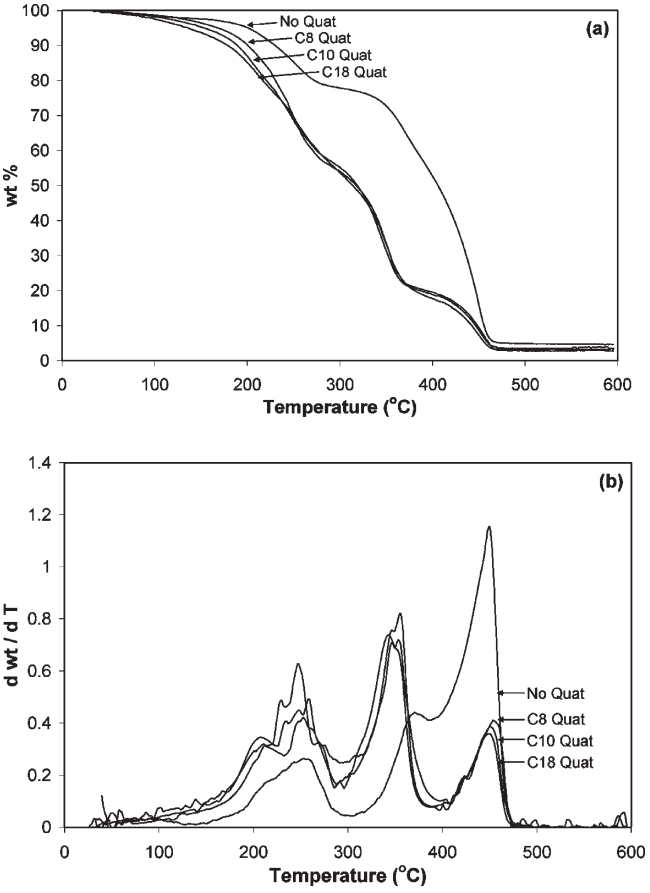

Figure 6. Thermogravimetric analysis of cured biocidal-urethane coatings, highlighting (a) thermal decomposition onset values and the (b) differential (dwt/dT) mass loss as a function of composition and temperature.

the film biocidal activity and suggests a stronger affinity between bacteria and the C8-containing coating.

Mechanical properties, extent of cross-linking and thermal stability of biocidal-urethane coatings were analyzed using DMA, gel factions, and TGA techniques, respectively. Results are summarized in Table 3. All samples had rubbery plateau modulus and glass transition (T_g) values characteristic of their composition, as was determined by DMA analysis in tensile mode utilizing the peak of the tan δ plot. Glass transitions were generally broad, indicating an inhomogeneous network structure, and show an interesting correlation with composition, Figure 4. DMA analysis reveals a plasticizing effect on the polymer network with the addition of the C8 (Figure 4b) alkyl chain relative to the unquaternized control (Figure 4a), as evidenced by the shifting peak maximum to lower temperatures. As the alkyl group length increases from C10 to C18 (Figure 4c,d), the plasticizing effect is lost,[37−40] and DMA analysis suggests that a phase-separated material results. Phase separation occurring on the microscale was further probed using AFM techniques. AFM analysis of the C18 QAS-urethane sample is presented in Figure 5 and supports a two-phase material, which may result from islands of QAS rich zones existing in a continuous phase of bulk polymer resin. The height plot (Figure 5, left) shows changes in topography, while the phase plot is representative of relative hardness over the sample area. Additional AFM analysis of other coatings prepared did not demonstrate phase-separated material, as suggested by the absence of the second transition in the DMA analysis.

The tan δ plot is often used to provide an indication of the dampening ability of the polymer network, which is related to the

material's ability to lose energy to molecular rearrangements and internal friction. There was significant dampening intensity in the tan δ plot observed in the series **5c**−**e** of >0.5 over a wide temperature range (approximately −10 to +40 °C). DMA analysis is suggestive for the potential multifunctional nature of these coatings (antimicrobial + damping); however, the frequency response of the damping and sound vibration dampening experiments are ongoing and will be reported as a separate study. Gel fractions were obtained for samples **5c**−**e**, as the insoluble mass fraction remaining after 24 h solvent exposure. The insoluble mass fraction remained high in all samples (>90 wt %), indicating the formation of extensive chemically cross-linked networks.

TGA was performed on cured samples **5c**−**e** and illustrated in Figure 6(a,b), and the initial onset of thermal degradation—temperature corresponding to 10 wt % mass loss—is provided in Table 3. As previously reported,[41] the presence of quaternary ammonium compounds served to reduce the thermal stability of polymer networks relative to unfunctionalized controls. The thermal degradation onset values are 200.6, 189.3, and 178.9 °C for quaternary ammonium alkyl chain lengths of C_8, C_{10}, and C_{18} respectively. Quaternary ammonium compounds are known to decompose through an initial Hoffmann elimination mechanism, thereby affording a volatile amine. Increased mass loss from C_{18} versus C_8 alkylated derivatives would be expected for each decomposition event, aiding in the observed trend in onset values. The wt % loss in samples, as described by Figure 6a, suggests a 3-phase thermal degradation profile of ∼200−300, 300−400, and 400−500 °C, which was further supported in the derivative plot, Figure 6b. Other than the variation of initial onset temperature with the structure of the alkyl group, little difference among the thermal stability of these samples **5c**−**e** was observed. Compared to nonquaternized controls, which show reduced mass loss over the first two decomposition stages, thermal analysis suggests that the quaternary alkyl group is not only readily cleaved at lower temperatures but the presence of this functionality accelerates the decomposition of base urethane resin. Additionally, early decomposition events may be attributed to the thermolysis of the linking urethane bonds, main-chain scission, and decomposition of the diol component.

4. CONCLUSIONS

Five alkyl diol-functionalized quaternary ammonium salts were synthesized and cross-linked within a resin to afford novel multifunctional self-decontaminating coatings. As a result of the amphiphilicity of the molecules, microphase separation as confirmed by AFM resulted, which also contributed to the desired viscoelastic properties of the resulting coating. Additionally, some of the coatings resulted in significant antimicrobial activity against multiple pathogenic bacteria. Based solely on the biocial activity of the coating 5c performs best; however, when other coating characteristics are considered including the potential for a multifunctional material having increased dampening characteristics, sample 5e may possess more intrinsic value.

AUTHOR INFORMATION

Corresponding Author

*Phone: (202) 404-4010. Fax:(202) 767-0594. E-mail: james.wynne@nrl.navy.mil.

Notes

[§]Formerly J. Paige Phillips.

REFERENCES

(1) Decraene, V.; Pratten, J.; Wilson, M. *Appl. Environ. Microbiol.* **2006**, *72*, 4436–4439.
(2) Punyani, S.; Singh, H. *J. Appl. Polym. Sci.* **2006**, *102*, 1038–1044.
(3) Nzeako, B. C.; Al Daughari, H.; Al Lamki, Z.; Al Rawas, O. *Br. J. Biomed. Sci.* **2006**, *63*, 55–58.
(4) Babu, R.; Zhang, J. Y.; Beckman, E. J.; Virji, M.; Pasculle, W. A.; Wells, A. *Biomaterials* **2006**, *27*, 4304–4314.
(5) Eby, D. M.; Luckarift, H. R.; Johnson, G. R. *ACS Appl. Mater. Interfaces* **2009**, *1*, 1553–1560.
(6) Hardes, J.; Ahrens, H.; Gebert, C.; Streitbuerger, A.; Buerger, H.; Erren, M.; Gunsel, A.; Wedemeyer, C.; Saxler, G.; Winkelmann, W.; Gosheger, G. *Biomaterials* **2007**, *28*, 2869–2875.
(7) Decraene, V.; Pratten, J.; Wilson, M. *Infect. Control Hosp. Epidemiol.* **2008**, *29*, 1181–1184.
(8) Decraene, V.; Pratten, J.; Wilson, M. *Curr. Microbiol.* **2008**, *57*, 269–273.
(9) Darouiche, R. O. *Clin. Infect. Dis.* **2003**, *36*, 1284–1289.
(10) Gollwitzer, H.; Thomas, P.; Diehl, P.; Steinhauser, E.; Summer, B.; Barnstorf, S.; Gerdesmeyer, L.; Mittelmeier, W.; Stemberger, A. *J. Orthop. Res.* **2005**, *23*, 802–809.
(11) Hilpert, K.; Elliott, M.; Jenssen, H.; Kindrachuk, J.; Fjell, C. D.; Korner, J.; Winkler, D. F. H.; Weaver, L. L.; Henklein, P.; Ulrich, A. S.; Chiang, S. H. Y.; Farmer, S. W.; Pante, N.; Volkmer, R.; Hancock, R. E. W. *Chem. Biol.* **2009**, *16*, 58–69.
(12) Statz, A. R.; Park, J. P.; Chongsiriwatana, N. P.; Barron, A. E.; Messersmith, P. B. *Biofouling* **2008**, *24*, 439–448.
(13) Fulmer, P. A.; Lundin, J. G.; Wynne, J. H. *ACS Appl. Mater. Interfaces* **2010**, *2*, 1266–1270.
(14) Harney, M. B.; Pant, R. R.; Fulmer, P. A.; Wynne, J. H. *ACS Appl. Mater. Interfaces* **2009**, *1*, 39–41.
(15) Pant, R. R.; Fulmer, P. A.; Harney, M. B.; Buckley, J. P.; Wynne, J. H. *J. Appl. Polym. Sci.* **2009**, *113*, 2397–2403.
(16) Pant, R. R.; Rasley, B. T.; Buckley, J. P.; Lloyd, C. T.; Cozzens, R. F.; Santangelo, P. G.; Wynne, J. H. *J. Appl. Polym. Sci.* **2007**, *104*, 2954–2964.
(17) McBain, A. J.; Ledder, R. G.; Moore, L. E.; Catrenich, C. E.; Gilbert, P. *Appl. Environ. Microbiol.* **2004**, *70*, 3449–3456.
(18) Hazzizalaskar, J.; Helary, G.; Sauvet, G. *J. Appl. Polym. Sci.* **1995**, *58*, 77–84.
(19) Pant, R. R.; Buckley, J. L.; Fulmer, P. A.; Wynne, J. H.; McCluskey, D. M.; Phillips, J. P. *J. Appl. Polym. Sci.* **2008**, *110*, 3080–3086.
(20) Majumdar, P.; Lee, E.; Gubbins, N.; Christianson, D. A.; Stafslien, S. J.; Daniels, J.; Vanderwal, L.; Bahr, J.; Chisholm, B. J. *J. Comb. Chem.* **2009**, *11*, 1115–27.
(21) Ye, S.; Majumdar, P.; Chisholm, B.; Stafslien, S.; Chen, Z. *Langmuir* 2010.
(22) Gottenbos, B.; van der Mei, H. C.; Klatter, F.; Nieuwenhuis, P.; Busscher, H. J. *Biomaterials* **2002**, *23*, 1417–1423.
(23) Sauvet, G.; Fortuniak, W.; Kazmierski, K.; Chojnowski, J. *J. Polym. Sci., Part A: Polym. Chem.* **2003**, *41*, 2939–2948.
(24) Hugo, W. B. *J. Appl. Bacteriol.* **1967**, *30*, 17–50.
(25) Tashiro, T. *Macromol. Mater. Eng.* **2001**, *286*, 63–87.
(26) Ahlstrom, B.; Thompson, R. A.; Edebo, L. *APMIS* **1999**, *107*, 318–24.
(27) Tomlinson, E.; Brown, M. R.; Davis, S. S. *J. Med. Chem.* **1977**, *20*, 1277–82.
(28) Ahmad, I.; Zaidi, J. H.; Hussain, R.; Munir, A. *Polym. Int.* **2007**, *56*, 1521–1529.
(29) Chang, W. H.; Scriven, R. L.; Peffer, J. R.; Porter, S. *Ind. Eng. Chem. Prod. Res. Dev.* **1973**, *12*, 278–288.
(30) Prabu, A. A.; Alagar, M. *J. Macromol. Sci., Pure Appl. Chem.* **2005**, *A42*, 175–188.
(31) Bruchmann, B. *Macromol. Mater. Eng.* **2007**, *292*, 981–992.
(32) Lee, B. H.; Choi, J. H.; Kim, H. J.; Kim, J. I.; Park, J. Y. *J. Ind. Eng. Chem.* **2004**, *10*, 608–613.
(33) Makal, U.; Wood, L.; Ohman, D. E.; Wynne, K. J. *Biomaterials* **2006**, *27*, 1316–1326.

(34) Tan, J.; Brash, J. L. *J. Appl. Polym. Sci.* **2008**, *108*, 1617–1628.
(35) McCluskey, D. M.; Smith, T. N.; Madasu, P. K.; Coumbe, C. E.; Mackey, M. A.; Fulmer, P. A.; Wynne, J. H.; Stevenson, S.; Phillips, J. P. *ACS Appl. Mater. Interfaces* **2009**, *1*, 882–887.
(36) Wynne, J. H.; Pant, R. R.; Jones-Meehan, J. M.; Phillips, J. P. *J. Appl. Polym. Sci.* **2008**, *107*, 2089–2094.
(37) Gao, S. J.; Zhang, L. N. *Macromolecules* **2001**, *34*, 2202–2207.
(38) Ghasemlou, M.; Khodaiyan, F.; Oromiehie, A. *Carbohydr. Polym.* **2011**, *84*, 477–483.
(39) Gozzelino, G.; Dell'Aquila, G. A.; Tobar, D. R. *J. Appl. Polym. Sci.* **2009**, *112*, 2334–2342.
(40) Kopesky, E. T.; Haddad, T. S.; McKinley, G. H.; Cohen, R. E. *Polymer* **2005**, *46*, 4743–4752.
(41) Pant, R. R.; Fulmer, P. A.; Wynne, J. H. *Abstracts of Papers, 237th ACS National Meeting* **2009**, *237*, PMSE–268.